

Minerva Access is the Institutional Repository of The University of Melbourne

Author/s:

Awuku, S;Bradley, SJ;Ghiggino, KP;Steer, RP;Stevens, AL;White, JM;Yeow, C

Title:

Photophysics and spectroscopy of 1,2-Benzazulene

Date:

2021-12

Citation:

Awuku, S., Bradley, S. J., Ghiggino, K. P., Steer, R. P., Stevens, A. L., White, J. M. & Yeow, C. (2021). Photophysics and spectroscopy of 1,2-Benzazulene. *Chemical Physics Letters*, 784, <https://doi.org/10.1016/j.cplett.2021.139114>.

Persistent Link:

<https://hdl.handle.net/11343/337707>

Accepted Version: Published in Chemical Physics Letters, Vol. 784, 139114 (2021); <https://doi.org/10.1016/j.cplett.2021.139114>

Photophysics and Spectroscopy of 1,2-Benzazulene

Stephen Awuku,^b Siobhan J. Bradley,^a Kenneth P. Ghiggino,^{a*} Ronald P. Steer,^{b*}

Amy L. Stevens,^{b*} Jonathan M. White,^a Colleen Yeow^a

^a School of Chemistry and ARC Centre of Excellence in Exciton Science
University of Melbourne
Parkville, VIC 3010, Australia

^b Department of Chemistry
University of Saskatchewan
Saskatoon, SK
Canada S7N5C9

*Authors to whom correspondence should be addressed.

*K. P. Ghiggino. E-mail: ghiggino@unimelb.edu.au.

*R. P. Steer. E-mail: ron.steer@usask.ca.

*A. L Stevens. Email: amy.stevens@usask.ca

Abstract

The electronic spectroscopy and photophysics of 1,2-benzazulene (BzAz) have been examined in solution and in thin solid films, with the objective of comparing its intramolecular and intermolecular excited state decay processes with those of azulene. Unlike azulene, the $S_2 - S_0$ absorption and fluorescence spectra exhibit a clear mirror image relationship dominated by a single strong Franck-Condon active progression. Picosecond transient absorption spectra and non-linear S_2 fluorescence upconversion experiments reveal lifetimes that follow a well-established energy gap law correlation, indicative of a dominant $S_2 - S_1$ decay route. Mechanistic interpretations, including the possibility of S_2 singlet fission in aggregates, are discussed.

Introduction

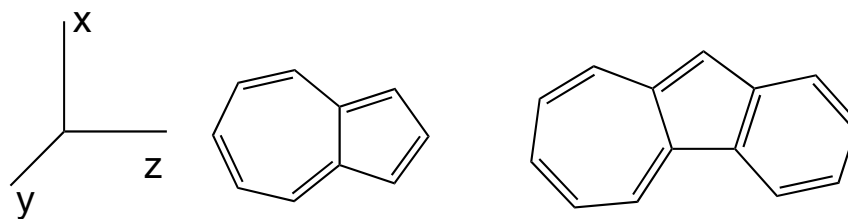
As documented in recent reviews,¹⁻⁵ azulene has received more attention in the photophysics and spectroscopy literature over the last seventy years than any other simple aromatic hydrocarbon. Azulene's nonalternant carbon framework results in uncommon electronic properties including an exceptionally large spacing between its first and second singlet excited states, $\Delta E(S_2 - S_1)$, due primarily to the weak interaction between its HOMO and LUMO electrons which generates a low-lying S_1 state. This and its structural stability result in an S_2 excited state that is exceptionally long-lived, leading to a readily detectable anomalous, "contra-Kasha" $S_2 - S_0$ fluorescence.^{6,7} The vibrational and vibronic spectroscopy of azulene have been investigated experimentally in considerable detail,⁸⁻¹⁰ with fulsome theoretical analyses and interpretation of its unusual features.^{9,11}

Recently, interest in the photophysics of azulene and its derivatives has been renewed because azulene could, on the basis of its electronic energy spacings, participate in singlet fission (SF) from S_2 in suitable bichromophoric materials;^{3,4,12} the $S_2 + S_0 \rightarrow 2T_1$ process is exoergic. This possibility was first recognized by Nickel and coworkers some thirty years ago,¹³ but SF in azulene itself has not been observed, possibly because of the unfavourable photophysical properties of its lower electronic states. Its first excited singlet state is very short-lived due to a conical potential energy surface intersection with S_0 , and its $S_1 - T_1$ electronic energy gap is small enough that thermally activated back-intersystem crossing from T_1 to S_1 reduces any triplet concentration at room temperature to barely detectable levels.

The possibility that azulene's derivatives might possess photophysical properties that circumvent these problems has not been pursued robustly, despite existing reports^{3,4} suggesting that some derivatives might be useful. Thus 1-fluoro- and 1,3-difluoroazulene possess even larger $\Delta E(S_2 - S_1)$ values than azulene itself, and the 1,3-difluoro derivative has an S_2 lifetime of almost 10 ns.¹⁴ Arene annulated derivatives such as benzo- and naphtho-azulene are known to fluoresce from S_2 ,^{15,16} but their photophysical properties have not been reported in detail. Nevertheless, on the basis of their basic electronic spectral characteristics, they too appear to be possible candidates for S_2 SF. Here we provide a detailed account of the photophysics and spectroscopy of 1,2-benzazulene in condensed media and assess its suitability for incorporation as the working S_2 SF chromophore in a suitably structured homo-bichromophoric material.

Experimental Section

Materials: The synthesis of 1,2-benzazulene (benz[a]azulene, BzAz), Scheme 1, was adapted from the procedure of Sperandio and Hansen.¹⁷ Details are provided in the Supporting Information. Azulene (Sigma-Aldrich) and zinc tetraphenylporphyrin (ZnTPP, Porphyrin Systems) were employed as reference materials, and were used as received. Solvents (toluene, Tol; methylcyclohexane, MCH; methanol, MeOH; stabilizer-free tetrahydrofuran, THF, Sigma-Aldrich) were of spectroscopic grade and were used without further purification. The coordinate system used to define the symmetry elements of the two compounds is shown in Scheme 1. Azulene's time averaged structure is taken to be described by the C_{2v} point group.



Scheme 1. Azulene (left) and 1,2-benzazulene (right).

Instrumentation: Solution absorbances and absorption spectra were measured using a Cary 6000i double beam spectrophotometer. Quartz cuvettes with path lengths between 10 mm and 0.1 mm (for highly concentrated samples) were used for the absorbance measurements. Steady-state fluorescence emission measurements were carried out using a PTI QuantaMaster double-grating spectrofluorometer. A custom-modified SPEX fluorometer fitted with 355, 405, and 561 nm cw excitation lasers and a set of calibrated neutral density filters to reduce the laser's power reaching the sample was also used. Notch filters were employed to remove scatter at the excitation wavelengths, and a 520 nm long-bandpass filter was put in place on the emission side in order to distinguish the observable second-order diffraction artifact from true fluorescence signals in the red and near infrared regions. Except for thin films, all fluorescence spectra were taken in 2 mm x 10 mm rectangular cuvettes or in a triangular front-face excitation cell to minimize self-absorption effects.

Transient absorption spectra of BzAz and their temporal rise and decay profiles were measured using 400 nm laser excitation and a delayed supercontinuum probe exhibiting a 150 fs FWHM instrument response function, as previously described.¹⁸

Temporal decay profiles of the $S_2 - S_0$ fluorescence of BzAz samples in various solvents were measured using non-linear fluorescence upconversion instrumentation described in detail by Tripathy, *et al.*¹⁹ The laser repetition rate was 10 kHz, while the detection wavelength was set at 435 nm, near the S_2 fluorescence emission peak. Scattering from pure toluene at 462 nm was used to determine the instrument response function of 380 fs (FWHM). The sample, placed in a 2 mm-path length cuvette, was continuously stirred during the experiment to minimize photolysis. In order to avoid photon-counting artifacts in the detection electronics, the upconverted fluorescence peak count rate was limited to $\leq 5\%$ of the laser's repetition rate.

Thin films of BzAz were obtained by drop-casting aliquots of a saturated solution of the sample in MCH on a quartz disk and slowly evaporating the solvent.

Results and Discussion

The photostability of BzAz was examined by exposing a small volume of a vigorously stirred 0.1mM aerated solution in toluene to 2.34 mW of 355 nm light from an unfocussed cw laser and following the changes in its $S_2 - S_0$ absorbance at 403.5 nm. Very small but reproducibly measurable continuous decreases in absorbance were noted over a period of 1 hour, as shown in Figure S1 (Supporting Information). The quantum yield of BzAz's photochemical consumption under these conditions was calculated to be 1×10^{-4} .

(a) Spectroscopy

The $S_1 - S_0$ and $S_2 - S_0$ absorption spectra of BzAz in several solvents at room temperature are shown in Figure 1. The best resolved spectra are obtained in non-

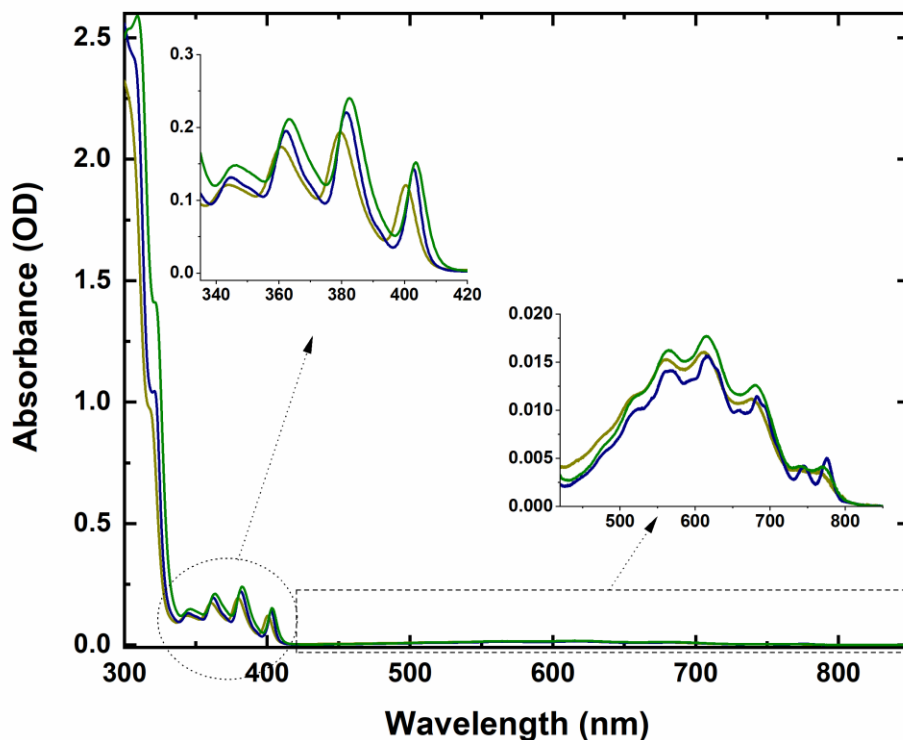


Figure 1: Absorption spectra of 50 μM BzAz in different solvents; methanol (dark yellow), methylcyclohexane (navy blue) and toluene (olive green) with insets amplifying the $S_2 - S_0$ (left) and $S_1 - S_0$ (right) electronic transitions.

polar MCH. Similar but less well vibronically-resolved spectra were also obtained in other solvents and are similar to those reported previously.^{15,20} At concentrations less than 0.01 M these spectra are independent of concentration in all solvents, indicative of a lack of observable ground state aggregation in dilute solution. Evidence of BzAz aggregation does appear as a broad feature in the 450 nm region in thin films of the compound on quartz (*cf.* Figure S2, Supplementary Information). The wavenumbers of the vibronic origin bands, which are red-shifted relative to azulene, and the $S_2 - S_1$ electronic energy gaps in these solvents are recorded in

Table 1. Assuming that the $S_1 - T_1$ electronic energy spacing in BzAz is similar to that of azulene itself,²¹ *i.e.* *ca.* 500 cm^{-1} , one concludes that the zero point energy of S_2 almost exactly equals $2E(T_1)$ in these solvents. Thus $S_2 + S_0 \rightarrow 2T_1$ SF, were it to occur, should be almost thermoneutral in a bichromophoric BzAz species.

Table 1: Data for the energies of the $S_2(2^1A')$ and $S_1(1^1A')$ states of BzAz from its absorption spectra in several solvents and its red-shifts relative to azulene.

solvent	$E(S_1)$ origin, cm^{-1}	$E(S_2)$ origin, cm^{-1}	$\Delta E(S_2 - S_1)$ cm^{-1}	$E(S_1)(\text{Az-BzAz})$ cm^{-1}	$E(S_2)(\text{Az-BzAz})$ cm^{-1}
MCH	12883	24826	11943	-	-
toluene	12998	24784	11786	1437	3502
methanol	13068	24976	11908	-	-

The $S_1 - S_0$ absorption spectrum of BzAz in solution is similar to those previously reported when the compound was first synthesized,^{15,20} and is similar to that of azulene itself in the same media.^{10,22} However, its $S_2 - S_0$ absorption system (Figure 1) differs significantly from that of azulene. Only one major vibronic progression is observed in these solution spectra and, unlike azulene, the origin band is strong and part of a regular Franck-Condon series from $v' = 0$ to $v' = 3$. The fundamental frequency of this vibration in S_2 is 1390 cm^{-1} . At higher energies the $S_2 - S_0$ vibronic system becomes overlapped by the stronger $S_3 - S_0$ absorption band.

The $S_2 - S_0$ fluorescence spectrum of BzAz in solution is readily observed when exciting at any energy in the near uv; that obtained by exciting in MCH in the $S_3 - S_0$ origin band at 320 nm, avoiding scatter, is shown in Figure 2. The spectrum

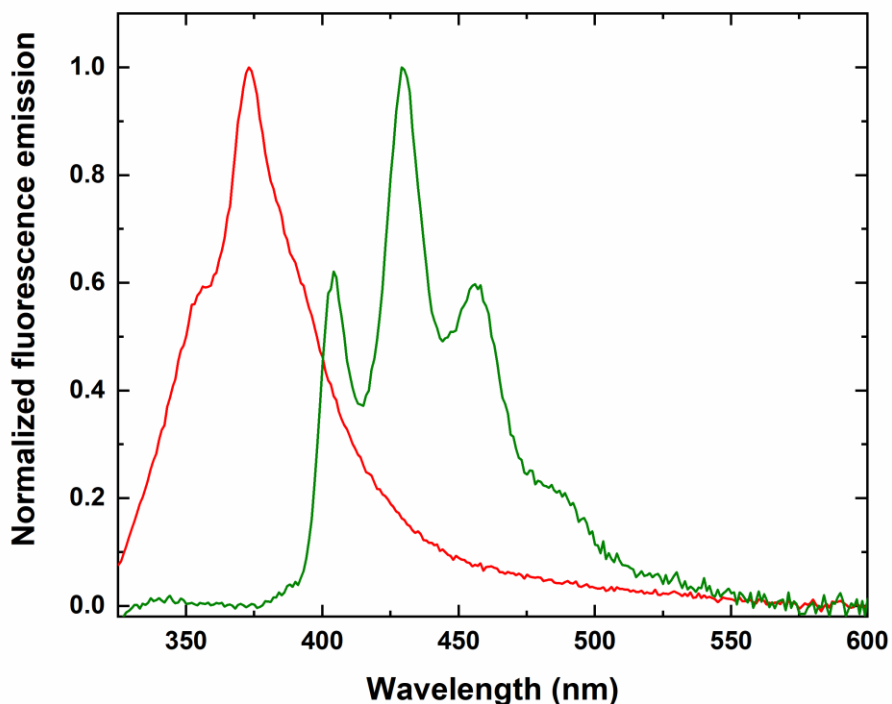


Figure 2: Comparison of the normalized, background corrected fluorescence spectra of BzAz (olive green) and azulene (red), both 10 μM in toluene excited at 320 nm under identical instrumental conditions.

resulting from exciting in the $S_2 - S_0$ origin band is shown in Figure S3 (Supporting Information). Unlike that of azulene itself, this fluorescence spectrum is a clear mirror image of the $S_2 - S_0$ absorption, and exhibits one distinct vibronic progression. The origin band of the fluorescence spectrum (obtained from the higher energy excitation) is located at 24784 cm^{-1} (in toluene), and the ground state fundamental frequency, estimated from the spacing between the $v'' = 1$ and $v'' = 0$ peaks in the emission spectrum, is 1450 cm^{-1} , slightly larger than that of its S_2 counterpart, as expected. This vibration is assigned to a totally symmetric in-plane ring stretching vibration on the basis of the ground state Raman spectrum of BzAz (*cf.*

Figures S4A and S4B, Supporting Information) in which the strongest band in the solid phase has a frequency of 1499 cm^{-1} .

Although only a few details about the vibrational structure of these $S_2 \leftrightarrow S_0$ spectra are available from solution phase measurements, it is nevertheless clear that there are significant differences between these BzAz spectra and the corresponding ones of azulene, which have been thoroughly examined in many media, including jet-cooled gas phase conditions at high resolution.^{8,9} In azulene (C_{2v} structure), the $S_2(1A_1) - S_0(1A_1)$ absorption, which is z polarized, gains much of its intensity by coupling of S_2 with $S_4(1A_1)$ via several totally symmetric a_1 skeletal vibrations.⁹ In BzAz, of lower C_s symmetry, one Raman active a' vibration dominates the vibronic structure in both the absorption and emission spectra. The result is a pair of $S_2(1A') \leftrightarrow S_0(1A')$ absorption and fluorescence spectra that are mirror images and that exhibit smooth progressions of band intensities. The vibronic intensity profiles of these spectra suggest that the equilibrium structure of the S_2 state of BzAz is more like that of its S_0 state than that displayed by azulene itself.

Like azulene, the $S_1 - S_0$ absorption spectrum of BzAz is weaker than its $S_2 - S_0$ counterpart, with an oscillator strength ratio, $f_{S_2}/f_{S_1} = 13:1$. In azulene this transition is to the S_1 state of B_1 symmetry, with a transition moment parallel to the transannular bond, consistent with the increased C(9)-C(10) bond strength in its excited state.²³ In BzAz the state symmetry change on excitation to S_1 is formally removed, but unlike the $S_2 - S_0$ system, the $S_1 - S_0$ transition retains its azulene-like character. Like azulene, the lowest frequency vibronic bands in BzAz's $S_1 - S_0$ spectrum (Figure 1) are somewhat weaker than those of the main progressions.^{8,22}

The lowest energy resolvable vibronic feature in these solution-phase absorption spectra is located 540 cm^{-1} from the origin, which correlates well with the low frequency a_1 vibrations of greatest intensity observed in the corresponding high resolution and solution-phase spectra of azulene. The remaining vibronic bands in the $S_1 - S_0$ spectrum of BzAz follow a general intensity pattern and have an overall spectral breadth similar to that of azulene in similar media. We conclude that, apart from stabilization of some 1440 cm^{-1} , fusion of the benzo group in the 1,2-position has only minor effects on the properties of the S_1 state of the chromophore.

Azulene exhibits very weak $S_2 - S_1$ fluorescence when excited in its $S_2 - S_0$ absorption bands,²⁴ and its $S_1 - S_0$ emission can be observed via thermally activated intersystem crossing from T_1 states produced initially by sensitization.²⁵ In the case of BzAz, only the second order grating diffraction signal of $S_2 - S_0$ fluorescence is observed in the expected $S_2 - S_1$ and $S_1 - S_0$ emission regions at $\lambda > 800\text{ nm}$ (*cf.* Figure S3, Supporting Information). Strong cw laser excitation of BzAz at wavelengths within its weaker $S_1 - S_0$ absorption system also produced no measurable S_1 fluorescence in room temperature solutions. On the basis of this absence of emission, we estimate the quantum yields of directly excited $S_2 - S_1$ and $S_1 - S_0$ fluorescence to be less than 3×10^{-7} .

(b) Photophysics

The S_2 fluorescence decay times of BzAz excited at 400 nm for several concentrations in three solvents were measured by the non-linear fluorescence upconversion technique. The temporal profiles of the fluorescence signals in these solvents and their fits to single exponential decay functions are shown in Figure 3.

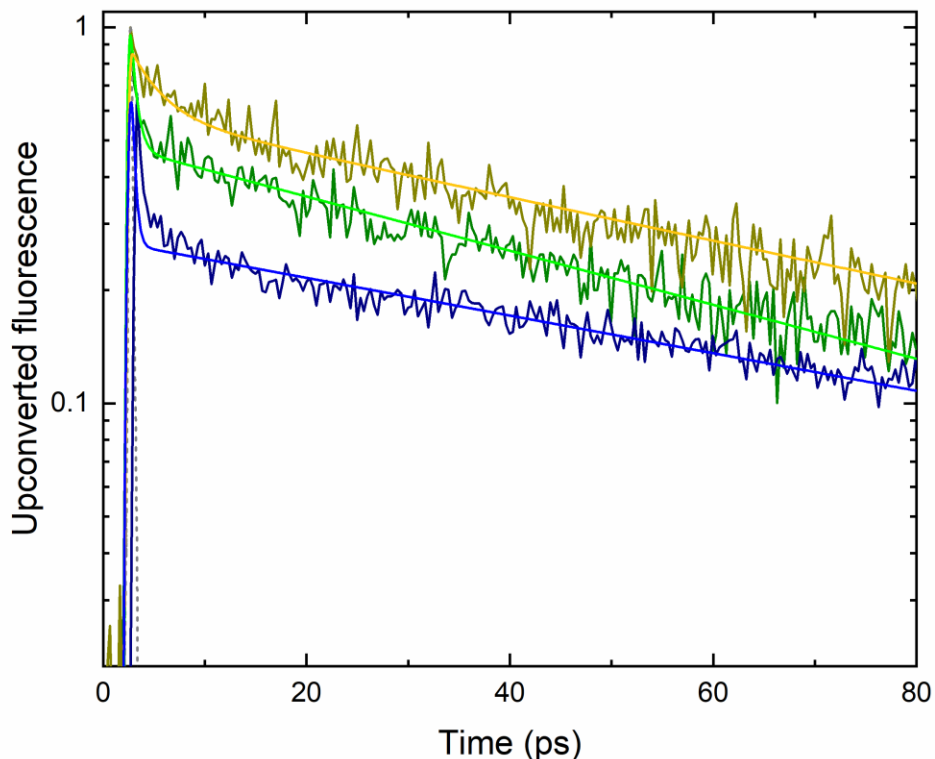


Figure 3: Upconverted S_2 fluorescence lifetime of $50 \mu\text{M}$ BzAz excited at 400 nm in methanol (dark yellow), methylcyclohexane (navy blue) and toluene (olive green), and monitored at 435 nm. The solid lines show the fit to the instrument response function (which includes solvent Raman scatter when observing at 435 nm) with single exponential fluorescence decay functions. The broken line shows the instrument response function curve determined at 462 nm.

The instrument response function at the 435 nm detection wavelength also contains signal due to solvent Raman scatter.

The time-resolved transient absorption spectra of BzAz in THF excited at 400 nm are shown in Figure 4. Fitting of the decays of the broad transient absorptions at several wavelengths in the 480 nm to 750 nm range to single exponential decay functions produce lifetimes of S_2 in THF of 65 ps (*cf.* Figure S5, Supporting Information), very similar to the decay times measured by fluorescence

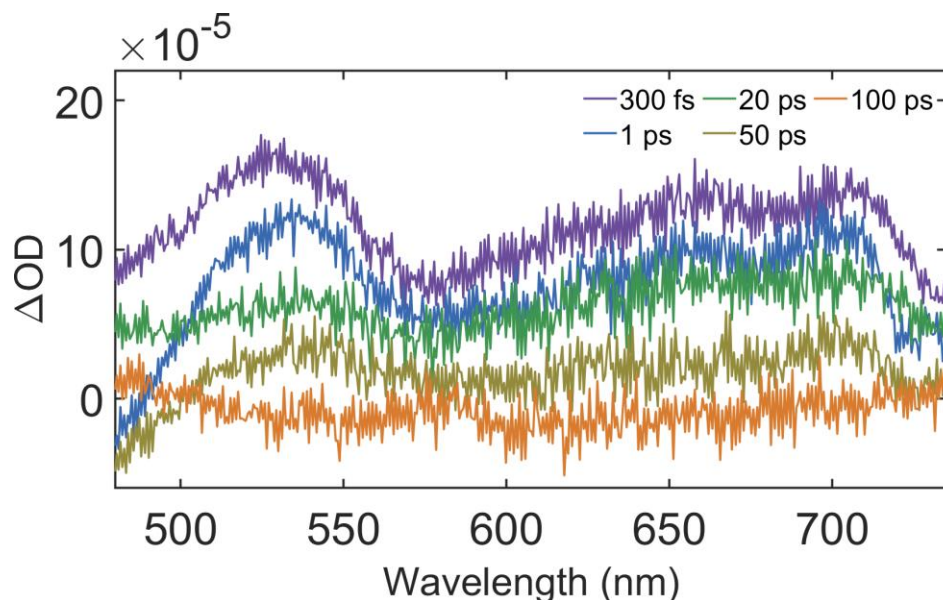


Figure 4: Transient absorption spectra of 0.46 mM BzAz excited at 400 nm in THF as a function of pump-probe delay time.

upconversion in similar polar solvents. The major features of these measurements are similar to those obtained by a transient grating technique for BzAz excited at 400 nm in acetonitrile and assigned to S_2 .²⁶ Excitation of BzAz at 400 nm populates vibrationally cold S_2 states, so together with its measured lifetimes, the assignment of this fluorescent transient to the S_2 state of BzAz in dilute solution is secure. The decay data obtained from both the fluorescence decay and transient absorption experiments are shown in Table 2.

Using ZnTPP in toluene as a reference (*cf.* Figure S6, Supporting Information) the $S_2 - S_0$ fluorescence quantum yield of BzAz in toluene excited in its origin band at 405 nm was measured to be $(2.0 \pm 0.1) \times 10^{-3}$. Together with an S_2 lifetime of 66 ps in the same solvent, these data yield a radiative decay rate constant,

Table 2: Kinetic parameters describing the radiative and non-radiative relaxation processes of the excited electronic states of BzAz in several solvents at room temperature.

BzAz	solvent	τ (ps)	ϕ_f	k_r (s ⁻¹)	Σk_{nr} (s ⁻¹)
S ₂	MCH	95 ± 5*			1.0x10 ¹⁰
	toluene	66	2.0x10 ⁻³	3.0x10 ⁷	1.5x10 ¹⁰
	methanol	68			1.5x10 ¹⁰
	acetonitrile**	74			1.4x10 ¹⁰
S ₁	MCH	-	<3x10 ⁻⁷		
	toluene	-	<3x10 ⁻⁷	2.0x10 ⁶	>8x10 ¹²

* average of 6 trials, extrapolated to infinitely dilute solution.

** from reference 26.

$k_{rS_2} = 3.0 \times 10^7 \text{ s}^{-1}$ and a sum of S₂ non-radiative first order decay constants, $\Sigma k_{nrS_2} = 1.5 \times 10^{10} \text{ s}^{-1}$ in toluene. These data and similar values in other solvents, are displayed in Table 2. There is no direct evidence of the non-radiative decay path of the S₂ state of BzAz in these measurements. However, there is a reasonable energy gap law correlation of BzAz's values of Σk_{nrS_2} at its measured $\Delta E(S_2 - S_1)$, with those of the S₂ states of other species exhibiting dominant S₂ - S₁ radiationless decay,³ including azulene and its fluorinated derivatives,^{14,27} as shown in Figure 5. This correlation suggests that the main non-radiative decay process of the S₂ state of BzAz is internal conversion to S₁, like the other species of Figure 5.

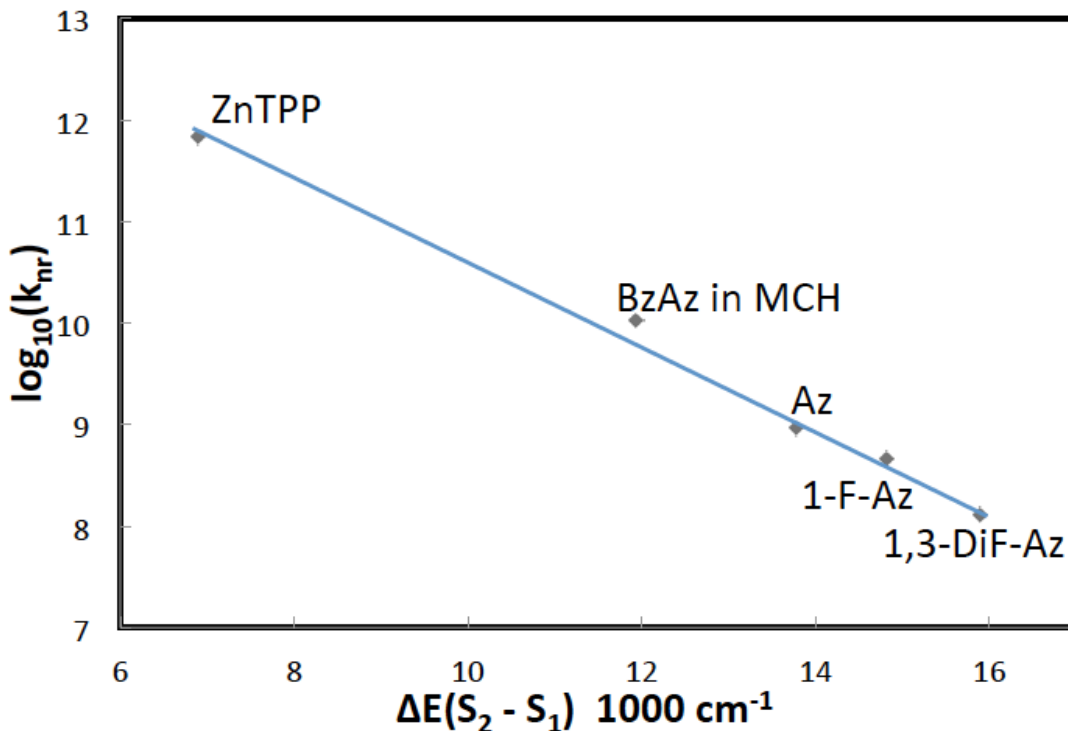


Figure 5: Energy gap law plot illustrating the correlation of the non-radiative decay rate of the S_2 state of BzAz with those of azulene, 1-fluoroazulene, 1,3-difluoroazulene and ZnTPP in toluene, all of which exhibit dominant $S_2 - S_1$ internal conversion. The BzAz data are in Tables 1 and 2.

BzAz is photostable, so its lack of observable $S_1 - S_0$ fluorescence following either $S_2 - S_1$ internal conversion or direct excitation to upper vibrational levels of S_1 suggests that, like azulene, the S_1 state undergoes ultrafast internal conversion to high vibrational levels of S_0 . Using the experimentally determined value of k_{rS_2} and the ratio of the oscillator strengths of the $S_2 - S_0$ and $S_1 - S_0$ absorptions of BzAz (*vide supra*), we calculate $k_{rS_1} = 2.0 \times 10^6 \text{ s}^{-1}$ for BzAz. An estimate of the upper limit of the $S_1 - S_0$ fluorescence quantum yield, $\phi_{fS_1} < 3 \times 10^{-7}$, then places the $S_1 - S_0$ radiationless decay rate constant of vibrationally hot S_1 states, k_{nrS_1} , to be greater than $8 \times 10^{12} \text{ s}^{-1}$. This is clearly faster than the intermolecular vibrational relaxation rates in solution, so we conclude that in dilute solution, like azulene, BzAz

undergoes ultrafast $S_1 - S_0$ internal conversion via conical intersection of the two singlet potential energy surfaces.

At BzAz concentrations near saturation (*ca.* 0.01M in MCH), there is no spectroscopic evidence of ground state aggregation, despite the reasonable probability of dipolar solute interactions that could be particularly significant in MCH. (Note, however, that the structures of azulene dimers are different from those expected on a simple dipolar interaction basis.²⁸) Furthermore there is only a slight, statistically weak indication of a decrease in the S_2 lifetime of BzAz in solution in concentration ranges up to saturation, consistent with self-quenching at a rate no greater than the diffusion controlled limit. $S_2 + S_0 \rightarrow 2 S_1$ FRET in solution is also eliminated on the basis of the very small quantum yield of $S_2 - S_1$ fluorescence and the weak $S_0 - S_1$ absorption. However, there is clear evidence of aggregation in the absorption spectra of thin films of pure BzAz, as shown in Figure S2 (Supporting Information). Excitation within and to the red of the monomer $S_0 - S_2$ absorption in these thin films produces almost no $S_2 - S_0$ fluorescence, indicative of a very rapid (subpicosecond) radiationless decay process in the amorphous solid that could include SF. There is, however, no evidence at this point of triplet formation under S_2 excitation in these films.

Conclusions

The electronic spectroscopy and photophysics of 1,2-benzazulene reveal interesting similarities to and differences from its azulene parent. The $S_1 - S_0$ absorption spectra of BzAz are similar to those of azulene in similar solvents. However, unlike azulene, its $S_2 - S_0$ absorption and fluorescence spectra exhibit a

clear mirror image relationship dominated by a single strong Franck-Condon active progression. Picosecond transient absorption spectra reveal a broad spectrum assignable to the S_2 state and non-linear S_2 fluorescence upconversion experiments reveal lifetimes that follow a well-established energy gap law correlation, indicating that the $S_2 - S_1$ decay route is dominant in BzAz as it is in azulene itself. However, neither $S_2 - S_1$ nor $S_1 - S_0$ fluorescence could be observed in BzAz, and its T_1 state could not be seen by transient absorption. These data suggest that, like azulene, BzAz undergoes ultrafast $S_1 - S_0$ radiationless decay by conical intersection of the potential surfaces at high S_0 vibrational energies, bypassing T_1 . Singlet fission (SF) from excited electronic states S_n ($n > 1$) in aggregates of polyatomic molecules has been observed recently in several systems.²⁹⁻³¹ In 1993 Nickel proposed that $S_2 + S_0 \rightarrow 2 T_1$ SF should occur in azulene and, like azulene, the electronic spectra of BzAz reveal that such an SF process would be near thermoneutral. However, evidence of neither aggregation nor ultrafast self-quenching of the S_2 state of BzAz was observed in solutions up to the solute saturation limits. Evidence of aggregation is seen in thin solid films of BzAz, but they provide almost no measurable S_2 fluorescence and no transient absorption signal assignable to T_1 . The BzAz S_2 exciton decay rate must therefore be ultrafast in these thin films, but the decay mechanism remains an open question.

Associated Content:

* Supporting Information

Detailed synthesis and characterization procedures for BzAz. Spectra showing the rate of photochemical consumption of BzAz in solution. Spectra of BzAz solid thin

films. Spectra showing the second order diffraction identity of features in the BzAz fluorescence spectrum. The Raman and FTIR spectra of BzAz. A typical BzAz S₂ transient absorption decay. Fluorescence spectra used to determine fluorescence quantum yields.

Author Information:

Corresponding Authors

*K. P. Ghiggino. E-mail: ghiggino@unimelb.edu.au.

*R. P. Steer. E-mail: ron.steer@usask.ca.

*A. L. Stevens. Email: amy.stevens@usask.ca

ORCID

Kenneth P. Ghiggino: 0000-0001-6621-4448

Ronald P. Steer: 0000-0003-2333-8218

Amy L. Stevens: 0000-0002-0998-1795

Jonathan M. White: 0000-0002-0707-6257

Colleen Yeow: 0000-0003-3496-0934

Notes:

The authors declare no competing financial interest.

Acknowledgements

The authors thank the Natural Sciences and Engineering Research Council of Canada and the Australian Research Council Centre of Excellence in Exciton Science (CE170100026) for their continuing financial support. The Saskatchewan Structural Science Centre provided equipment and technical assistance. Thanks to George Belev.

References

- (1) Prlj, A.; Begušić, T.; Zhang, Z. T.; Fish, G. C.; Wehrle, M.; Zimmermann, T.; Choi, S.; Roulet, J.; Moser, J.-E.; Vaníček, J. Semiclassical Approach to Photophysics Beyond Kasha's Rule and Vibronic Spectroscopy Beyond the Condon Approximation. The Case of Azulene. *J. Chem. Theory Comput.* **2020**, *16*, 2617–2626.
- (2) Ou, L.; Zhou, Y.; Wu, B.; Zhu, L. The Unusual Physicochemical Properties of Azulene and Azulene-Based Compounds. *Chin. Chem. Lett.* **2019**, *30*, 1903–1907.
- (3) Steer, R. P. Photophysics of Molecules Containing Multiples of the Azulene Carbon Framework. *J. Photochem. Photobiol. C* **2019**, *40*, 68–80.
- (4) Xin, H.; Gao, X. Application of Azulene in Constructing Organic Optoelectronic Materials: New Tricks for an Old Dog. *ChemPlusChem* **2017**, *82*, 945–956.
- (5) Liu, R. S. H.; Asato, A. E. Tuning the Color and Excited State Properties of the Azulenic Chromophore: NIR Absorbing Pigments and Materials. *J. Photochem. Photobiol. C* **2003**, *4*, 179–194.
- (6) Demchenko, A. P.; Tomin, V. I.; Chou, P.-T. Breaking the Kasha Rule for More Efficient Photochemistry. *Chem. Rev.* **2017**, *117*, 13353–13381.
- (7) Itoh, T. Fluorescence and Phosphorescence from Higher Excited States of Organic Molecules. *Chem. Rev.* **2012**, *112*, 4541–4568.
- (8) Ruth, A. A.; Kim, E.-K.; Hese, A. The $S_0 \rightarrow S_1$ Cavity Ring-Down Absorption Spectrum of Jet-Cooled Azulene: Dependence of Internal Conversion on the Excess Energy. *Phys. Chem. Chem. Phys.* **1999**, *1*, 5121–5128.
- (9) Lawrance, W. D.; Knight, A. E. Unraveling of Vibronically Scrambled Electronic

Spectra: The S₂-S₀ Transition in Azulene. *J. Phys. Chem.* **1990**, *94*, 1249–1267.

(10) Lu, H. M.; Page, J. B. On the use of Combination/Overtone Band Resonance Raman Excitation Profiles for Understanding the Vibronic Coupling Mechanism in the 700 nm Absorption Band of Azulene. *J. Chem. Phys.* **1990**, *92*, 7038–7049.

(11) Brafman, O.; Chan, C. K.; Khodadoost, B.; Page, J. B.; Walker, C. T. Resonance Raman Scattering Study of Azulene. I. Experiment and Theoretical Analysis Via Transform Techniques. *J. Chem. Phys.* **1984**, *80*, 5406–5417.

(12) Stevens, A. L.; Yeow, C.; White, J. M.; Bradley, S. J.; Ghiggino, K. P.; Steer, R. P. Electronic Spectroscopy and Photophysics of Calix[4]azulene. *J. Photochem. Photobiol. A* **2021**, *405*, 112922.

(13) Nickel, B.; Klemp, D. The Lowest Triplet State of Azulene-*h*₈ and Azulene-*d*₈ in Liquid Solution. I. Survey, Kinetic Considerations, Experimental Technique, and Temperature Dependence of Triplet Decay. *Chem. Phys.* **1993**, *174*, 297–318.

(14) Tétreault, N.; Muthyala, R. S.; Liu, R. S. H.; Steer, R. P. Control of the Photophysical Properties of Polyatomic Molecules by Substitution and Solvation: The Second Excited Singlet State of Azulene. *J. Phys. Chem. A* **1999**, *103*, 2524–2531.

(15) Yamaguchi, H.; Ninomiya, K.; Fukuda, M.; Muraoka, T. Magnetic Circular dichroism and Anomalous Fluorescence Spectra of Benz[a]azulene and Naphth[2,1-a]azulene. *Spectrochim. Acta*, **1980**, *36A*, 1003–1005.

(16) Yamaguchi, H.; Sato, S.; Yasunam, M.; Sato, T.; Yoshinobu, M. Anomalous Fluorescence Spectra of Benz[a]azulene Derivatives. *Spectrochim. Acta A* **1997**, *53*, 2471–2473.

- (17) Sperandio, D.; Hansen, H.-J. An Efficient Straightforward Synthesis of Benz[a]azulene. *Helv. Chim. Acta*, 1995, **78**, 765–771, and references therein.
- (18) Bradley, S. J.; Chi, M.; White, J. M.; Hall, C. R.; Goerigk, L.; Smith, T. A.; Ghiggino, K. P. The Role of Conformational Heterogeneity in the Excited State Dynamics of Linked Diketopyrrolopyrrole Dimers. *Phys. Chem. Chem. Phys.*, **2021**, *23*, 9357-9364.
- (19) Tripathy, U.; Kowalska, D.; Liu, X.; Velate, S.; Steer, R. P. Photophysics of Soret-Excited Tetrapyrroles in Solution. I. Metalloporphyrins: MgTPP, ZnTPP, and CdTPP. *J. Phys. Chem. A* **2008**, *112*, 5824–5833.
- (20) Nunn, J. R.; Rapson, W. S. Cyclic Conjugated Polyenes. Part I. 1,2-Benzazulene. *J. Chem. Soc.* **1949**, 825-83.
- (21) Vosskötter, S.; Konieczny, P.; Marian, C. M.; Weinkauff, R. Towards an Understanding of the Singlet–Triplet Splittings in Conjugated Hydrocarbons: Azulene Investigated by Anion Photoelectron Spectroscopy and Theoretical Calculations. *Phys. Chem. Chem. Phys.* **2015**, *17*, 23573–23581.
- (22) Lou, Y.; Chang, J.; Jorgensen, J.; Lemal, D. M. Octachloroazulene. *J. Am. Chem. Soc.* **2002**, *124*, 15302–15307.
- (23) Bearpark, M.; Bernardi, F.; Clifford, S.; Olivucci, M.; Robb, M. A.; Smith, B. R.; Vreven, T. The Azulene S_1 State Decays via a Conical Intersection: A CASSCF Study with MMVB Dynamics. *J. Am. Chem. Soc.* **1996**, *118*, 169–175.
- (24) Klemp, D.; Nickel, B. Relative Quantum Yield of the $S_2 \rightarrow S_1$ Fluorescence from Azulene. *Chem. Phys. Lett.* **1986**, *130*, 493–497.

- (25) Nickel, B.; Klemp, D. The Lowest Triplet State of Azulene-h₈ and Azulene-d₈ in Liquid Solution. II. Phosphorescence and E-Type Delayed Fluorescence. *Chem. Phys.* **1993**, *174*, 319–330.
- (26) Muller, P.-A.; Vauthey, E. Charge Recombination Dynamics of Geminate Ion Pairs Formed by Electron Transfer Quenching of Molecules in an Upper Excited State. *J. Phys. Chem. A* **2001**, *105*, 5994–6000.
- (27) Wagner, B. D.; Tittelbach-Helmrich, D.; Steer, R. P. Radiationless Decay of the S₂ States of Azulene and Related Compounds: Solvent Dependence and the Energy Gap Law. *J. Phys. Chem.* **1992**, *96*, 7904–7908.
- (28) Piacenza, M.; Grimme, S. Van der Waals Complexes of Polar Aromatic Molecules: Unexpected Structures for Dimers of Azulene, *J. Amer. Chem. Soc.* **2005**, *127*, 14841–14848.
- (29) Ma, L.; Zhang, K.; Kloc, C.; Sun, H.; Michel-Beyerle, M. E.; Gurzadyan, G. G. Singlet Fission in Rubrene Single Crystal: Direct Observation by Femtosecond Pump-Probe Spectroscopy. *Phys. Chem. Chem. Phys.* **2012**, *14*, 8307–8312.
- (30) Ni, W.; Gurzadyan, G. G.; Ma, L.; Hu, P.; Kloc, C.; Sun, L. Ultrafast Tuning of Various Photochemical Pathways in Perylene–TCNQ Charge-Transfer Crystals. *J. Phys. Chem. C* **2020**, *124*, 13894–13901.
- (31) Zhao, T.; Kloc, C.; Ni, W.; Sun, L.; Gurzadyan, G. G. Revealing ultrafast relaxation dynamics in six-thiophene thin film and single crystal. *J. Photochem. Photobiol. A* **2021**, *404*, 112920.

Photophysics and Spectroscopy of 1,2-Benzazulene

Stephen Awuku,^b Siobhan J. Bradley,^a Kenneth P. Ghiggino,^{a*} Ronald P. Steer,^{b*}

Amy L. Stevens,^{b*} Jonathan M. White,^a Colleen Yeow^a

^a School of Chemistry and ARC Centre of Excellence in Exciton Science
University of Melbourne
Parkville, VIC 3010, Australia

^b Department of Chemistry
University of Saskatchewan
Saskatoon, SK
Canada S7N5C9

*Authors to whom correspondence should be addressed.

*K. P. Ghiggino. E-mail: ghiggino@unimelb.edu.au.

*R. P. Steer. E-mail: ron.steer@usask.ca.

*A. L Stevens. Email: amy.stevens@usask.ca

Abstract

The electronic spectroscopy and photophysics of 1,2-benzazulene (BzAz) have been examined in solution and in thin solid films, with the objective of comparing its intramolecular and intermolecular excited state decay processes with those of azulene. Unlike azulene, the $S_2 - S_0$ absorption and fluorescence spectra exhibit a clear mirror image relationship dominated by a single strong Franck-Condon active progression. Picosecond transient absorption spectra and non-linear S_2 fluorescence upconversion experiments reveal lifetimes that follow a well-established energy gap law correlation, indicative of a dominant $S_2 - S_1$ decay route. Mechanistic interpretations, including the possibility of S_2 singlet fission in aggregates, are discussed.

Introduction

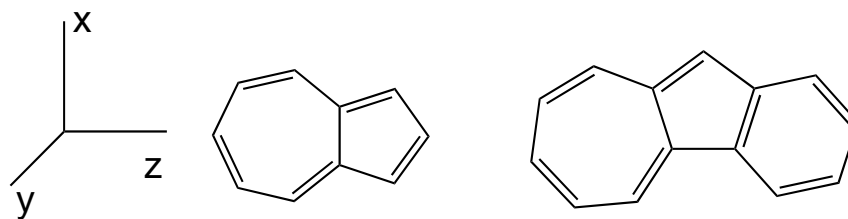
As documented in recent reviews,¹⁻⁵ azulene has received more attention in the photophysics and spectroscopy literature over the last seventy years than any other simple aromatic hydrocarbon. Azulene's nonalternant carbon framework results in uncommon electronic properties including an exceptionally large spacing between its first and second singlet excited states, $\Delta E(S_2 - S_1)$, due primarily to the weak interaction between its HOMO and LUMO electrons which generates a low-lying S_1 state. This and its structural stability result in an S_2 excited state that is exceptionally long-lived, leading to a readily detectable anomalous, "contra-Kasha" $S_2 - S_0$ fluorescence.^{6,7} The vibrational and vibronic spectroscopy of azulene have been investigated experimentally in considerable detail,⁸⁻¹⁰ with fulsome theoretical analyses and interpretation of its unusual features.^{9,11}

Recently, interest in the photophysics of azulene and its derivatives has been renewed because azulene could, on the basis of its electronic energy spacings, participate in singlet fission (SF) from S_2 in suitable bichromophoric materials;^{3,4,12} the $S_2 + S_0 \rightarrow 2T_1$ process is exoergic. This possibility was first recognized by Nickel and coworkers some thirty years ago,¹³ but SF in azulene itself has not been observed, possibly because of the unfavourable photophysical properties of its lower electronic states. Its first excited singlet state is very short-lived due to a conical potential energy surface intersection with S_0 , and its $S_1 - T_1$ electronic energy gap is small enough that thermally activated back-intersystem crossing from T_1 to S_1 reduces any triplet concentration at room temperature to barely detectable levels.

The possibility that azulene's derivatives might possess photophysical properties that circumvent these problems has not been pursued robustly, despite existing reports^{3,4} suggesting that some derivatives might be useful. Thus 1-fluoro- and 1,3-difluoroazulene possess even larger $\Delta E(S_2 - S_1)$ values than azulene itself, and the 1,3-difluoro derivative has an S_2 lifetime of almost 10 ns.¹⁴ Arene annulated derivatives such as benzo- and naphtho-azulene are known to fluoresce from S_2 ,^{15,16} but their photophysical properties have not been reported in detail. Nevertheless, on the basis of their basic electronic spectral characteristics, they too appear to be possible candidates for S_2 SF. Here we provide a detailed account of the photophysics and spectroscopy of 1,2-benzazulene in condensed media and assess its suitability for incorporation as the working S_2 SF chromophore in a suitably structured homo-bichromophoric material.

Experimental Section

Materials: The synthesis of 1,2-benzazulene (benz[a]azulene, BzAz), Scheme 1, was adapted from the procedure of Sperandio and Hansen.¹⁷ Details are provided in the Supporting Information. Azulene (Sigma-Aldrich) and zinc tetraphenylporphyrin (ZnTPP, Porphyrin Systems) were employed as reference materials, and were used as received. Solvents (toluene, Tol; methylcyclohexane, MCH; methanol, MeOH; stabilizer-free tetrahydrofuran, THF, Sigma-Aldrich) were of spectroscopic grade and were used without further purification. The coordinate system used to define the symmetry elements of the two compounds is shown in Scheme 1. Azulene's time averaged structure is taken to be described by the C_{2v} point group.



Scheme 1. Azulene (left) and 1,2-benzazulene (right).

Instrumentation: Solution absorbances and absorption spectra were measured using a Cary 6000i double beam spectrophotometer. Quartz cuvettes with path lengths between 10 mm and 0.1 mm (for highly concentrated samples) were used for the absorbance measurements. Steady-state fluorescence emission measurements were carried out using a PTI QuantaMaster double-grating spectrofluorometer. A custom-modified SPEX fluorometer fitted with 355, 405, and 561 nm cw excitation lasers and a set of calibrated neutral density filters to reduce the laser's power reaching the sample was also used. Notch filters were employed to remove scatter at the excitation wavelengths, and a 520 nm long-bandpass filter was put in place on the emission side in order to distinguish the observable second-order diffraction artifact from true fluorescence signals in the red and near infrared regions. Except for thin films, all fluorescence spectra were taken in 2 mm x 10 mm rectangular cuvettes or in a triangular front-face excitation cell to minimize self-absorption effects.

Transient absorption spectra of BzAz and their temporal rise and decay profiles were measured using 400 nm laser excitation and a delayed supercontinuum probe exhibiting a 150 fs FWHM instrument response function, as previously described.¹⁸

Temporal decay profiles of the $S_2 - S_0$ fluorescence of BzAz samples in various solvents were measured using non-linear fluorescence upconversion instrumentation described in detail by Tripathy, *et al.*¹⁹ The laser repetition rate was 10 kHz, while the detection wavelength was set at 435 nm, near the S_2 fluorescence emission peak. Scattering from pure toluene at 462 nm was used to determine the instrument response function of 380 fs (FWHM). The sample, placed in a 2 mm-path length cuvette, was continuously stirred during the experiment to minimize photolysis. In order to avoid photon-counting artifacts in the detection electronics, the upconverted fluorescence peak count rate was limited to $\leq 5\%$ of the laser's repetition rate.

Thin films of BzAz were obtained by drop-casting aliquots of a saturated solution of the sample in MCH on a quartz disk and slowly evaporating the solvent.

Results and Discussion

The photostability of BzAz was examined by exposing a small volume of a vigorously stirred 0.1mM aerated solution in toluene to 2.34 mW of 355 nm light from an unfocussed cw laser and following the changes in its $S_2 - S_0$ absorbance at 403.5 nm. Very small but reproducibly measurable continuous decreases in absorbance were noted over a period of 1 hour, as shown in Figure S1 (Supporting Information). The quantum yield of BzAz's photochemical consumption under these conditions was calculated to be 1×10^{-4} .

(a) Spectroscopy

The $S_1 - S_0$ and $S_2 - S_0$ absorption spectra of BzAz in several solvents at room temperature are shown in Figure 1. The best resolved spectra are obtained in non-

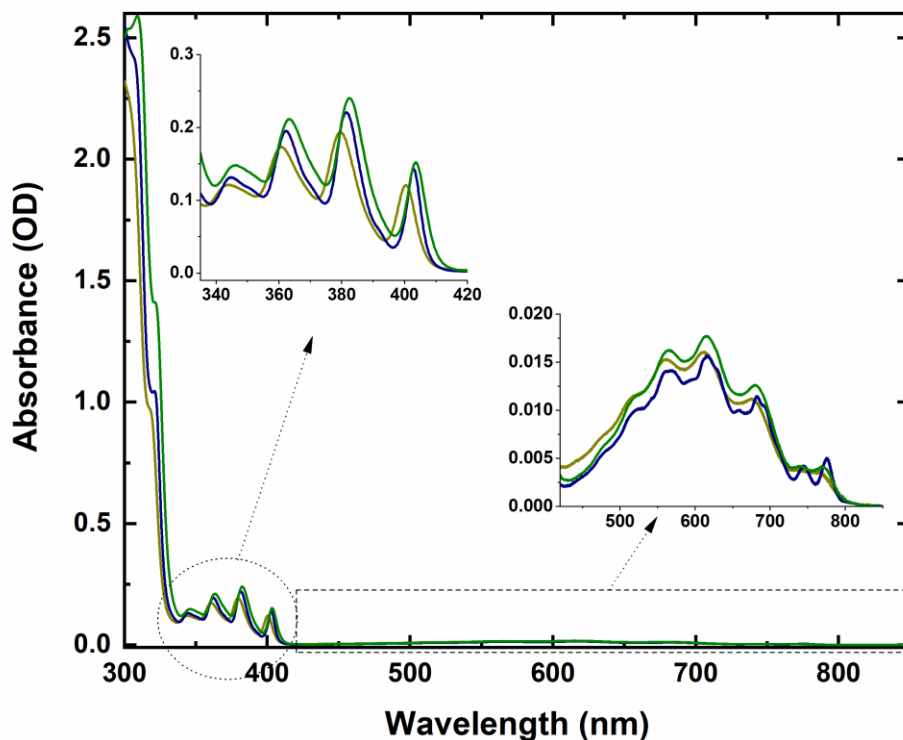


Figure 1: Absorption spectra of 50 μM BzAz in different solvents; methanol (dark yellow), methylcyclohexane (navy blue) and toluene (olive green) with insets amplifying the $S_2 - S_0$ (left) and $S_1 - S_0$ (right) electronic transitions.

polar MCH. Similar but less well vibronically-resolved spectra were also obtained in other solvents and are similar to those reported previously.^{15,20} At concentrations less than 0.01 M these spectra are independent of concentration in all solvents, indicative of a lack of observable ground state aggregation in dilute solution. Evidence of BzAz aggregation does appear as a broad feature in the 450 nm region in thin films of the compound on quartz (*cf.* Figure S2, Supplementary Information). The wavenumbers of the vibronic origin bands, which are red-shifted relative to azulene, and the $S_2 - S_1$ electronic energy gaps in these solvents are recorded in

Table 1. Assuming that the $S_1 - T_1$ electronic energy spacing in BzAz is similar to that of azulene itself,²¹ *i.e.* *ca.* 500 cm^{-1} , one concludes that the zero point energy of S_2 almost exactly equals $2E(T_1)$ in these solvents. Thus $S_2 + S_0 \rightarrow 2T_1$ SF, were it to occur, should be almost thermoneutral in a bichromophoric BzAz species.

Table 1: Data for the energies of the $S_2(2^1A')$ and $S_1(1^1A')$ states of BzAz from its absorption spectra in several solvents and its red-shifts relative to azulene.

solvent	$E(S_1)$ origin, cm^{-1}	$E(S_2)$ origin, cm^{-1}	$\Delta E(S_2 - S_1)$ cm^{-1}	$E(S_1)(\text{Az-BzAz})$ cm^{-1}	$E(S_2)(\text{Az-BzAz})$ cm^{-1}
MCH	12883	24826	11943	-	-
toluene	12998	24784	11786	1437	3502
methanol	13068	24976	11908	-	-

The $S_1 - S_0$ absorption spectrum of BzAz in solution is similar to those previously reported when the compound was first synthesized,^{15,20} and is similar to that of azulene itself in the same media.^{10,22} However, its $S_2 - S_0$ absorption system (Figure 1) differs significantly from that of azulene. Only one major vibronic progression is observed in these solution spectra and, unlike azulene, the origin band is strong and part of a regular Franck-Condon series from $v' = 0$ to $v' = 3$. The fundamental frequency of this vibration in S_2 is 1390 cm^{-1} . At higher energies the $S_2 - S_0$ vibronic system becomes overlapped by the stronger $S_3 - S_0$ absorption band.

The $S_2 - S_0$ fluorescence spectrum of BzAz in solution is readily observed when exciting at any energy in the near uv; that obtained by exciting in MCH in the $S_3 - S_0$ origin band at 320 nm, avoiding scatter, is shown in Figure 2. The spectrum

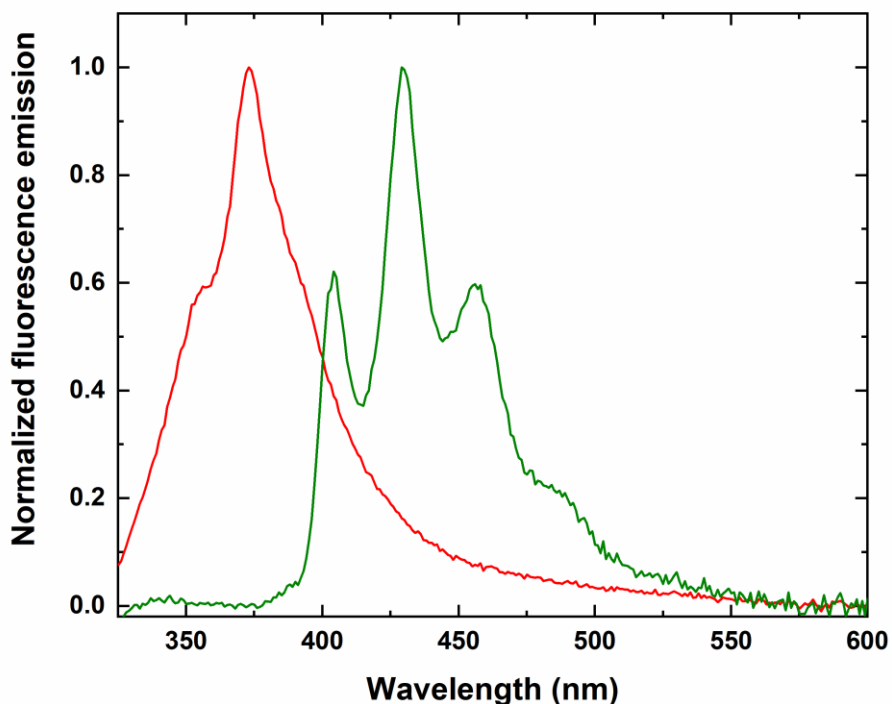


Figure 2: Comparison of the normalized, background corrected fluorescence spectra of BzAz (olive green) and azulene (red), both 10 μM in toluene excited at 320 nm under identical instrumental conditions.

resulting from exciting in the $S_2 - S_0$ origin band is shown in Figure S3 (Supporting Information). Unlike that of azulene itself, this fluorescence spectrum is a clear mirror image of the $S_2 - S_0$ absorption, and exhibits one distinct vibronic progression. The origin band of the fluorescence spectrum (obtained from the higher energy excitation) is located at 24784 cm^{-1} (in toluene), and the ground state fundamental frequency, estimated from the spacing between the $v'' = 1$ and $v'' = 0$ peaks in the emission spectrum, is 1450 cm^{-1} , slightly larger than that of its S_2 counterpart, as expected. This vibration is assigned to a totally symmetric in-plane ring stretching vibration on the basis of the ground state Raman spectrum of BzAz (*cf.*

Figures S4A and S4B, Supporting Information) in which the strongest band in the solid phase has a frequency of 1499 cm^{-1} .

Although only a few details about the vibrational structure of these $S_2 \leftrightarrow S_0$ spectra are available from solution phase measurements, it is nevertheless clear that there are significant differences between these BzAz spectra and the corresponding ones of azulene, which have been thoroughly examined in many media, including jet-cooled gas phase conditions at high resolution.^{8,9} In azulene (C_{2v} structure), the $S_2(1A_1) - S_0(1A_1)$ absorption, which is z polarized, gains much of its intensity by coupling of S_2 with $S_4(1A_1)$ via several totally symmetric a_1 skeletal vibrations.⁹ In BzAz, of lower C_s symmetry, one Raman active a' vibration dominates the vibronic structure in both the absorption and emission spectra. The result is a pair of $S_2(1A') \leftrightarrow S_0(1A')$ absorption and fluorescence spectra that are mirror images and that exhibit smooth progressions of band intensities. The vibronic intensity profiles of these spectra suggest that the equilibrium structure of the S_2 state of BzAz is more like that of its S_0 state than that displayed by azulene itself.

Like azulene, the $S_1 - S_0$ absorption spectrum of BzAz is weaker than its $S_2 - S_0$ counterpart, with an oscillator strength ratio, $f_{S_2}/f_{S_1} = 13:1$. In azulene this transition is to the S_1 state of B_1 symmetry, with a transition moment parallel to the transannular bond, consistent with the increased C(9)-C(10) bond strength in its excited state.²³ In BzAz the state symmetry change on excitation to S_1 is formally removed, but unlike the $S_2 - S_0$ system, the $S_1 - S_0$ transition retains its azulene-like character. Like azulene, the lowest frequency vibronic bands in BzAz's $S_1 - S_0$ spectrum (Figure 1) are somewhat weaker than those of the main progressions.^{8,22}

The lowest energy resolvable vibronic feature in these solution-phase absorption spectra is located 540 cm^{-1} from the origin, which correlates well with the low frequency a_1 vibrations of greatest intensity observed in the corresponding high resolution and solution-phase spectra of azulene. The remaining vibronic bands in the $S_1 - S_0$ spectrum of BzAz follow a general intensity pattern and have an overall spectral breadth similar to that of azulene in similar media. We conclude that, apart from stabilization of some 1440 cm^{-1} , fusion of the benzo group in the 1,2-position has only minor effects on the properties of the S_1 state of the chromophore.

Azulene exhibits very weak $S_2 - S_1$ fluorescence when excited in its $S_2 - S_0$ absorption bands,²⁴ and its $S_1 - S_0$ emission can be observed via thermally activated intersystem crossing from T_1 states produced initially by sensitization.²⁵ In the case of BzAz, only the second order grating diffraction signal of $S_2 - S_0$ fluorescence is observed in the expected $S_2 - S_1$ and $S_1 - S_0$ emission regions at $\lambda > 800\text{ nm}$ (*cf.* Figure S3, Supporting Information). Strong cw laser excitation of BzAz at wavelengths within its weaker $S_1 - S_0$ absorption system also produced no measurable S_1 fluorescence in room temperature solutions. On the basis of this absence of emission, we estimate the quantum yields of directly excited $S_2 - S_1$ and $S_1 - S_0$ fluorescence to be less than 3×10^{-7} .

(b) Photophysics

The S_2 fluorescence decay times of BzAz excited at 400 nm for several concentrations in three solvents were measured by the non-linear fluorescence upconversion technique. The temporal profiles of the fluorescence signals in these solvents and their fits to single exponential decay functions are shown in Figure 3.

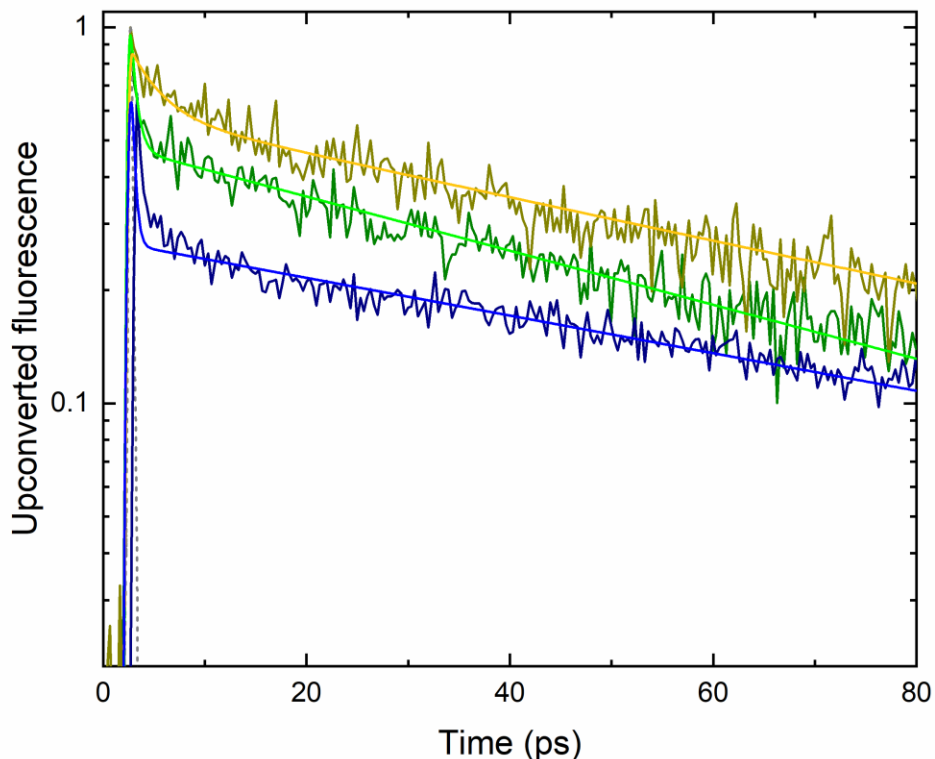


Figure 3: Upconverted S_2 fluorescence lifetime of 50 μM BzAz excited at 400 nm in methanol (dark yellow), methylcyclohexane (navy blue) and toluene (olive green), and monitored at 435 nm. The solid lines show the fit to the instrument response function (which includes solvent Raman scatter when observing at 435 nm) with single exponential fluorescence decay functions. The broken line shows the instrument response function curve determined at 462 nm.

The instrument response function at the 435 nm detection wavelength also contains signal due to solvent Raman scatter.

The time-resolved transient absorption spectra of BzAz in THF excited at 400 nm are shown in Figure 4. Fitting of the decays of the broad transient absorptions at several wavelengths in the 480 nm to 750 nm range to single exponential decay functions produce lifetimes of S_2 in THF of 65 ps (*cf.* Figure S5, Supporting Information), very similar to the decay times measured by fluorescence

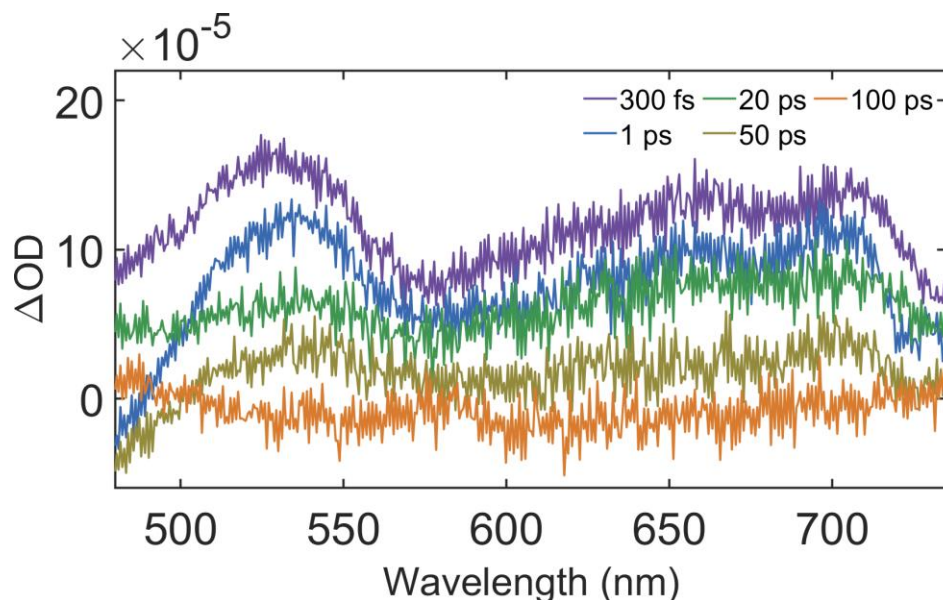


Figure 4: Transient absorption spectra of 0.46 mM BzAz excited at 400 nm in THF as a function of pump-probe delay time.

upconversion in similar polar solvents. The major features of these measurements are similar to those obtained by a transient grating technique for BzAz excited at 400 nm in acetonitrile and assigned to S_2 .²⁶ Excitation of BzAz at 400 nm populates vibrationally cold S_2 states, so together with its measured lifetimes, the assignment of this fluorescent transient to the S_2 state of BzAz in dilute solution is secure. The decay data obtained from both the fluorescence decay and transient absorption experiments are shown in Table 2.

Using ZnTPP in toluene as a reference (*cf.* Figure S6, Supporting Information) the $S_2 - S_0$ fluorescence quantum yield of BzAz in toluene excited in its origin band at 405 nm was measured to be $(2.0 \pm 0.1) \times 10^{-3}$. Together with an S_2 lifetime of 66 ps in the same solvent, these data yield a radiative decay rate constant,

Table 2: Kinetic parameters describing the radiative and non-radiative relaxation processes of the excited electronic states of BzAz in several solvents at room temperature.

BzAz	solvent	τ (ps)	ϕ_f	k_r (s ⁻¹)	Σk_{nr} (s ⁻¹)
S ₂	MCH	95 ± 5*			1.0x10 ¹⁰
	toluene	66	2.0x10 ⁻³	3.0x10 ⁷	1.5x10 ¹⁰
	methanol	68			1.5x10 ¹⁰
	acetonitrile**	74			1.4x10 ¹⁰
S ₁	MCH	-	<3x10 ⁻⁷		
	toluene	-	<3x10 ⁻⁷	2.0x10 ⁶	>8x10 ¹²

* average of 6 trials, extrapolated to infinitely dilute solution.

** from reference 26.

$k_{rS_2} = 3.0 \times 10^7 \text{ s}^{-1}$ and a sum of S₂ non-radiative first order decay constants, $\Sigma k_{nrS_2} = 1.5 \times 10^{10} \text{ s}^{-1}$ in toluene. These data and similar values in other solvents, are displayed in Table 2. There is no direct evidence of the non-radiative decay path of the S₂ state of BzAz in these measurements. However, there is a reasonable energy gap law correlation of BzAz's values of Σk_{nrS_2} at its measured $\Delta E(S_2 - S_1)$, with those of the S₂ states of other species exhibiting dominant S₂ - S₁ radiationless decay,³ including azulene and its fluorinated derivatives,^{14,27} as shown in Figure 5. This correlation suggests that the main non-radiative decay process of the S₂ state of BzAz is internal conversion to S₁, like the other species of Figure 5.

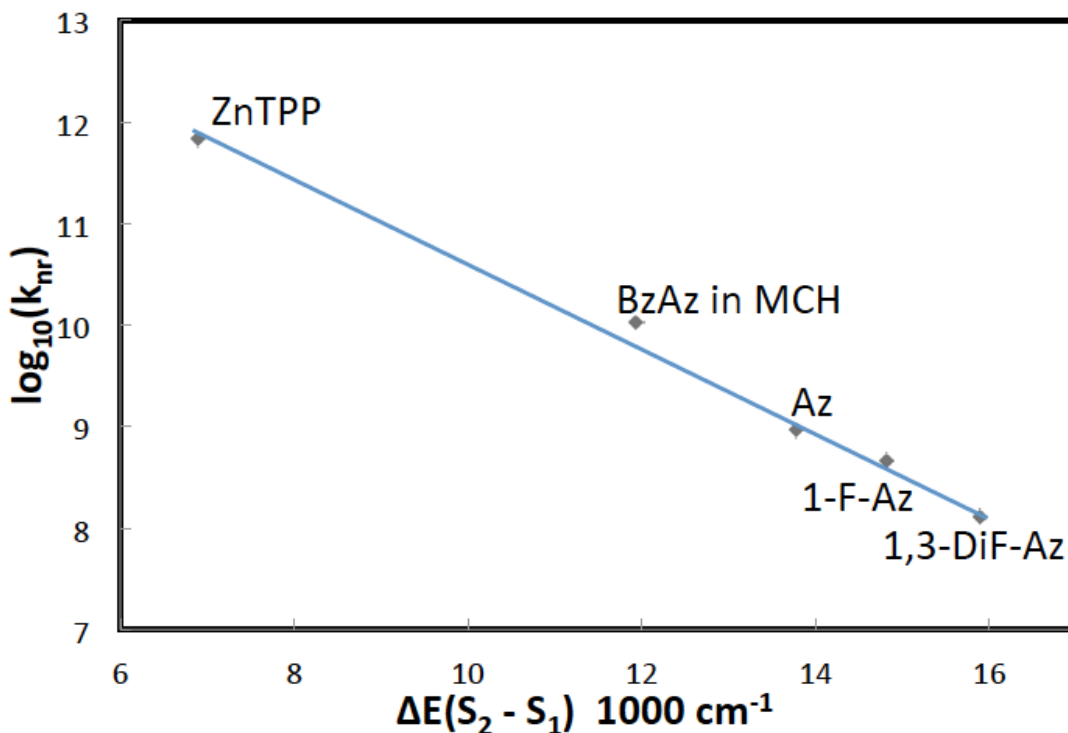


Figure 5: Energy gap law plot illustrating the correlation of the non-radiative decay rate of the S_2 state of BzAz with those of azulene, 1-fluoroazulene, 1,3-difluoroazulene and ZnTPP in toluene, all of which exhibit dominant $S_2 - S_1$ internal conversion. The BzAz data are in Tables 1 and 2.

BzAz is photostable, so its lack of observable $S_1 - S_0$ fluorescence following either $S_2 - S_1$ internal conversion or direct excitation to upper vibrational levels of S_1 suggests that, like azulene, the S_1 state undergoes ultrafast internal conversion to high vibrational levels of S_0 . Using the experimentally determined value of k_{rS_2} and the ratio of the oscillator strengths of the $S_2 - S_0$ and $S_1 - S_0$ absorptions of BzAz (*vide supra*), we calculate $k_{rS_1} = 2.0 \times 10^6 \text{ s}^{-1}$ for BzAz. An estimate of the upper limit of the $S_1 - S_0$ fluorescence quantum yield, $\phi_{fS_1} < 3 \times 10^{-7}$, then places the $S_1 - S_0$ radiationless decay rate constant of vibrationally hot S_1 states, k_{nrS_1} , to be greater than $8 \times 10^{12} \text{ s}^{-1}$. This is clearly faster than the intermolecular vibrational relaxation rates in solution, so we conclude that in dilute solution, like azulene, BzAz

undergoes ultrafast $S_1 - S_0$ internal conversion via conical intersection of the two singlet potential energy surfaces.

At BzAz concentrations near saturation (*ca.* 0.01M in MCH), there is no spectroscopic evidence of ground state aggregation, despite the reasonable probability of dipolar solute interactions that could be particularly significant in MCH. (Note, however, that the structures of azulene dimers are different from those expected on a simple dipolar interaction basis.²⁸) Furthermore there is only a slight, statistically weak indication of a decrease in the S_2 lifetime of BzAz in solution in concentration ranges up to saturation, consistent with self-quenching at a rate no greater than the diffusion controlled limit. $S_2 + S_0 \rightarrow 2 S_1$ FRET in solution is also eliminated on the basis of the very small quantum yield of $S_2 - S_1$ fluorescence and the weak $S_0 - S_1$ absorption. However, there is clear evidence of aggregation in the absorption spectra of thin films of pure BzAz, as shown in Figure S2 (Supporting Information). Excitation within and to the red of the monomer $S_0 - S_2$ absorption in these thin films produces almost no $S_2 - S_0$ fluorescence, indicative of a very rapid (subpicosecond) radiationless decay process in the amorphous solid that could include SF. There is, however, no evidence at this point of triplet formation under S_2 excitation in these films.

Conclusions

The electronic spectroscopy and photophysics of 1,2-benzazulene reveal interesting similarities to and differences from its azulene parent. The $S_1 - S_0$ absorption spectra of BzAz are similar to those of azulene in similar solvents. However, unlike azulene, its $S_2 - S_0$ absorption and fluorescence spectra exhibit a

clear mirror image relationship dominated by a single strong Franck-Condon active progression. Picosecond transient absorption spectra reveal a broad spectrum assignable to the S_2 state and non-linear S_2 fluorescence upconversion experiments reveal lifetimes that follow a well-established energy gap law correlation, indicating that the $S_2 - S_1$ decay route is dominant in BzAz as it is in azulene itself. However, neither $S_2 - S_1$ nor $S_1 - S_0$ fluorescence could be observed in BzAz, and its T_1 state could not be seen by transient absorption. These data suggest that, like azulene, BzAz undergoes ultrafast $S_1 - S_0$ radiationless decay by conical intersection of the potential surfaces at high S_0 vibrational energies, bypassing T_1 . Singlet fission (SF) from excited electronic states S_n ($n > 1$) in aggregates of polyatomic molecules has been observed recently in several systems.²⁹⁻³¹ In 1993 Nickel proposed that $S_2 + S_0 \rightarrow 2 T_1$ SF should occur in azulene and, like azulene, the electronic spectra of BzAz reveal that such an SF process would be near thermoneutral. However, evidence of neither aggregation nor ultrafast self-quenching of the S_2 state of BzAz was observed in solutions up to the solute saturation limits. Evidence of aggregation is seen in thin solid films of BzAz, but they provide almost no measurable S_2 fluorescence and no transient absorption signal assignable to T_1 . The BzAz S_2 exciton decay rate must therefore be ultrafast in these thin films, but the decay mechanism remains an open question.

Associated Content:

* Supporting Information

Detailed synthesis and characterization procedures for BzAz. Spectra showing the rate of photochemical consumption of BzAz in solution. Spectra of BzAz solid thin

films. Spectra showing the second order diffraction identity of features in the BzAz fluorescence spectrum. The Raman and FTIR spectra of BzAz. A typical BzAz S₂ transient absorption decay. Fluorescence spectra used to determine fluorescence quantum yields.

Author Information:

Corresponding Authors

*K. P. Ghiggino. E-mail: ghiggino@unimelb.edu.au.

*R. P. Steer. E-mail: ron.steer@usask.ca.

*A. L. Stevens. Email: amy.stevens@usask.ca

ORCID

Kenneth P. Ghiggino: 0000-0001-6621-4448

Ronald P. Steer: 0000-0003-2333-8218

Amy L. Stevens: 0000-0002-0998-1795

Jonathan M. White: 0000-0002-0707-6257

Colleen Yeow: 0000-0003-3496-0934

Notes:

The authors declare no competing financial interest.

Acknowledgements

The authors thank the Natural Sciences and Engineering Research Council of Canada and the Australian Research Council Centre of Excellence in Exciton Science (CE170100026) for their continuing financial support. The Saskatchewan Structural Science Centre provided equipment and technical assistance. Thanks to George Belev.

References

- (1) Prlj, A.; Begušić, T.; Zhang, Z. T.; Fish, G. C.; Wehrle, M.; Zimmermann, T.; Choi, S.; Roulet, J.; Moser, J.-E.; Vaníček, J. Semiclassical Approach to Photophysics Beyond Kasha's Rule and Vibronic Spectroscopy Beyond the Condon Approximation. The Case of Azulene. *J. Chem. Theory Comput.* **2020**, *16*, 2617–2626.
- (2) Ou, L.; Zhou, Y.; Wu, B.; Zhu, L. The Unusual Physicochemical Properties of Azulene and Azulene-Based Compounds. *Chin. Chem. Lett.* **2019**, *30*, 1903–1907.
- (3) Steer, R. P. Photophysics of Molecules Containing Multiples of the Azulene Carbon Framework. *J. Photochem. Photobiol. C* **2019**, *40*, 68–80.
- (4) Xin, H.; Gao, X. Application of Azulene in Constructing Organic Optoelectronic Materials: New Tricks for an Old Dog. *ChemPlusChem* **2017**, *82*, 945–956.
- (5) Liu, R. S. H.; Asato, A. E. Tuning the Color and Excited State Properties of the Azulenic Chromophore: NIR Absorbing Pigments and Materials. *J. Photochem. Photobiol. C* **2003**, *4*, 179–194.
- (6) Demchenko, A. P.; Tomin, V. I.; Chou, P.-T. Breaking the Kasha Rule for More Efficient Photochemistry. *Chem. Rev.* **2017**, *117*, 13353–13381.
- (7) Itoh, T. Fluorescence and Phosphorescence from Higher Excited States of Organic Molecules. *Chem. Rev.* **2012**, *112*, 4541–4568.
- (8) Ruth, A. A.; Kim, E.-K.; Hese, A. The $S_0 \rightarrow S_1$ Cavity Ring-Down Absorption Spectrum of Jet-Cooled Azulene: Dependence of Internal Conversion on the Excess Energy. *Phys. Chem. Chem. Phys.* **1999**, *1*, 5121–5128.
- (9) Lawrance, W. D.; Knight, A. E. Unraveling of Vibronically Scrambled Electronic

Spectra: The S₂-S₀ Transition in Azulene. *J. Phys. Chem.* **1990**, *94*, 1249–1267.

(10) Lu, H. M.; Page, J. B. On the use of Combination/Overtone Band Resonance Raman Excitation Profiles for Understanding the Vibronic Coupling Mechanism in the 700 nm Absorption Band of Azulene. *J. Chem. Phys.* **1990**, *92*, 7038–7049.

(11) Brafman, O.; Chan, C. K.; Khodadoost, B.; Page, J. B.; Walker, C. T. Resonance Raman Scattering Study of Azulene. I. Experiment and Theoretical Analysis Via Transform Techniques. *J. Chem. Phys.* **1984**, *80*, 5406–5417.

(12) Stevens, A. L.; Yeow, C.; White, J. M.; Bradley, S. J.; Ghiggino, K. P.; Steer, R. P. Electronic Spectroscopy and Photophysics of Calix[4]azulene. *J. Photochem. Photobiol. A* **2021**, *405*, 112922.

(13) Nickel, B.; Klemp, D. The Lowest Triplet State of Azulene-*h*₈ and Azulene-*d*₈ in Liquid Solution. I. Survey, Kinetic Considerations, Experimental Technique, and Temperature Dependence of Triplet Decay. *Chem. Phys.* **1993**, *174*, 297–318.

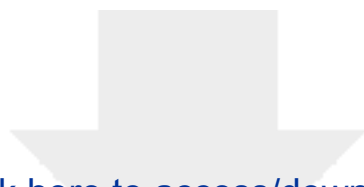
(14) Tétreault, N.; Muthyala, R. S.; Liu, R. S. H.; Steer, R. P. Control of the Photophysical Properties of Polyatomic Molecules by Substitution and Solvation: The Second Excited Singlet State of Azulene. *J. Phys. Chem. A* **1999**, *103*, 2524–2531.

(15) Yamaguchi, H.; Ninomiya, K.; Fukuda, M.; Muraoka, T. Magnetic Circular dichroism and Anomalous Fluorescence Spectra of Benz[a]azulene and Naphth[2,1-a]azulene. *Spectrochim. Acta*, **1980**, *36A*, 1003–1005.

(16) Yamaguchi, H.; Sato, S.; Yasunam, M.; Sato, T.; Yoshinobu, M. Anomalous Fluorescence Spectra of Benz[a]azulene Derivatives. *Spectrochim. Acta A* **1997**, *53*, 2471–2473.

- (17) Sperandio, D.; Hansen, H.-J. An Efficient Straightforward Synthesis of Benz[a]azulene. *Helv. Chim. Acta*, 1995, **78**, 765–771, and references therein.
- (18) Bradley, S. J.; Chi, M.; White, J. M.; Hall, C. R.; Goerigk, L.; Smith, T. A.; Ghiggino, K. P. The Role of Conformational Heterogeneity in the Excited State Dynamics of Linked Diketopyrrolopyrrole Dimers. *Phys. Chem. Chem. Phys.*, **2021**, *23*, 9357-9364.
- (19) Tripathy, U.; Kowalska, D.; Liu, X.; Velate, S.; Steer, R. P. Photophysics of Soret-Excited Tetrapyrroles in Solution. I. Metalloporphyrins: MgTPP, ZnTPP, and CdTPP. *J. Phys. Chem. A* **2008**, *112*, 5824–5833.
- (20) Nunn, J. R.; Rapson, W. S. Cyclic Conjugated Polyenes. Part I. 1,2-Benzazulene. *J. Chem. Soc.* **1949**, 825-83.
- (21) Vosskötter, S.; Konieczny, P.; Marian, C. M.; Weinkauff, R. Towards an Understanding of the Singlet–Triplet Splittings in Conjugated Hydrocarbons: Azulene Investigated by Anion Photoelectron Spectroscopy and Theoretical Calculations. *Phys. Chem. Chem. Phys.* **2015**, *17*, 23573–23581.
- (22) Lou, Y.; Chang, J.; Jorgensen, J.; Lemal, D. M. Octachloroazulene. *J. Am. Chem. Soc.* **2002**, *124*, 15302–15307.
- (23) Bearpark, M.; Bernardi, F.; Clifford, S.; Olivucci, M.; Robb, M. A.; Smith, B. R.; Vreven, T. The Azulene S₁ State Decays via a Conical Intersection: A CASSCF Study with MMVB Dynamics. *J. Am. Chem. Soc.* **1996**, *118*, 169–175.
- (24) Klemp, D.; Nickel, B. Relative Quantum Yield of the S₂ → S₁ Fluorescence from Azulene. *Chem. Phys. Lett.* **1986**, *130*, 493–497.

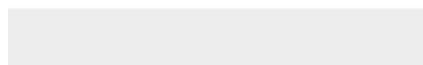
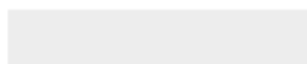
- (25) Nickel, B.; Klemp, D. The Lowest Triplet State of Azulene-h₈ and Azulene-d₈ in Liquid Solution. II. Phosphorescence and E-Type Delayed Fluorescence. *Chem. Phys.* **1993**, *174*, 319–330.
- (26) Muller, P.-A.; Vauthey, E. Charge Recombination Dynamics of Geminate Ion Pairs Formed by Electron Transfer Quenching of Molecules in an Upper Excited State. *J. Phys. Chem. A* **2001**, *105*, 5994–6000.
- (27) Wagner, B. D.; Tittelbach-Helmrich, D.; Steer, R. P. Radiationless Decay of the S₂ States of Azulene and Related Compounds: Solvent Dependence and the Energy Gap Law. *J. Phys. Chem.* **1992**, *96*, 7904–7908.
- (28) Piacenza, M.; Grimme, S. Van der Waals Complexes of Polar Aromatic Molecules: Unexpected Structures for Dimers of Azulene, *J. Amer. Chem. Soc.* **2005**, *127*, 14841–14848.
- (29) Ma, L.; Zhang, K.; Kloc, C.; Sun, H.; Michel-Beyerle, M. E.; Gurzadyan, G. G. Singlet Fission in Rubrene Single Crystal: Direct Observation by Femtosecond Pump-Probe Spectroscopy. *Phys. Chem. Chem. Phys.* **2012**, *14*, 8307–8312.
- (30) Ni, W.; Gurzadyan, G. G.; Ma, L.; Hu, P.; Kloc, C.; Sun, L. Ultrafast Tuning of Various Photochemical Pathways in Perylene–TCNQ Charge-Transfer Crystals. *J. Phys. Chem. C* **2020**, *124*, 13894–13901.
- (31) Zhao, T.; Kloc, C.; Ni, W.; Sun, L.; Gurzadyan, G. G. Revealing ultrafast relaxation dynamics in six-thiophene thin film and single crystal. *J. Photochem. Photobiol. A* **2021**, *404*, 112920.



[Click here to access/download](#)

Supplementary Materials

Awuku et al BzAz Supporting Information Oct 1.docx



Declaration of interests

The authors declare that they have no known competing financial interests or personal relationships that could have appeared to influence the work reported in this paper.

The authors declare the following financial interests/personal relationships which may be considered as potential competing interests:

The authors declare that they have no known competing financial or personal relationships that could have appeared to influence the work reported in this paper.

R. P. Steer
Corresponding author

Credit author statement

S. Awuku carried out many of the experiments, S. Bradley carried out the transient absorption experiments, K. P. Ghiggino supervised research at the University of Melbourne, R. P. Steer cosupervised research at the University of Saskatchewan, A. L. Stevens cosupervised research at the University of Saskatchewan, J. M. White supervised syntheses, C. Yeow carried out syntheses. All authors participated in writing the paper.